Evolutionary novelty in the apoptotic pathway of aphids

Mélanie Ribeiro Lopes[a], Nicolas Parisot[a], Karen Gaget[a], Cissy Huygens[b], Sergio Peignier[a], Gabrielle Duport[a], Julien Orlans[a], Hubert Charles[a], Pieter Baatsen[c], Emmanuelle Jousselin[d], Pedro Da Silva[a], Korneel Hens[e], Patrick Callaerts[b,1], and Federica Calevro[a,1]

[a]UMR0203, Biologie Fonctionnelle, Insectes et Interactions (BF2i), Institut National des Sciences Appliquées Lyon (INSA Lyon), Institut National de Recherche pour l'Agriculture, l'Alimentation et l'Environnement (INRAE), University of Lyon (Univ Lyon), F-69621 Villeurbanne, France; [b]Laboratory of Behavioral and Developmental Genetics, Department of Human Genetics, Katholieke Universiteit (KU) Leuven, University of Leuven, B-3000 Leuven, Belgium; [c]Center for Brain and Disease Research, VIB-KU Leuven, B-3000, Leuven, Belgium; [d]UMR 1062 Centre de Biologie pour la Gestion des Populations (CBGP), Institut National de Recherche pour l'Agriculture, l'Alimentation et l'Environnement (INRAE), Centre de coopération Internationale en Recherche Agronomique pour le Développement (CIRAD), Institut de Recherche pour le Développement (IRD), Montpellier SupAgro, Université de Montpellier, F- 34988 Montferrier sur Lez, France; and [e]Department of Biological and Medical Sciences, Centre for Functional Genomics, Oxford Brookes University, Oxford, OX3 OBP, United Kingdom

Edited by Trudy F. C. Mackay, Clemson University, Raleigh, NC, and approved November 3, 2020 (received for review July 8, 2020)

Apoptosis, a conserved form of programmed cell death, shows interspecies differences that may reflect evolutionary diversification and adaptation, a notion that remains largely untested. Among insects, the most speciose animal group, the apoptotic pathway has only been fully characterized in *Drosophila melanogaster*, and apoptosis-related proteins have been studied in a few other dipteran and lepidopteran species. Here, we studied the apoptotic pathway in the aphid *Acyrthosiphon pisum*, an insect pest belonging to the Hemiptera, an earlier-diverging and distantly related order. We combined phylogenetic analyses and conserved domain identification to annotate the apoptotic pathway in *A. pisum* and found low caspase diversity and a large expansion of its inhibitory part, with 28 inhibitors of apoptosis (IAPs). We analyzed the spatiotemporal expression of a selected set of pea aphid IAPs and showed that they are differentially expressed in different life stages and tissues, suggesting functional diversification. Five IAPs are specifically induced in bacteriocytes, the specialized cells housing symbiotic bacteria, during their cell death. We demonstrated the antiapoptotic role of these five IAPs using heterologous expression in a tractable in vivo model, the *Drosophila melanogaster* developing eye. Interestingly, IAPs with the strongest antiapoptotic potential contain two BIR and two RING domains, a domain association that has not been observed in any other species. We finally analyzed all available aphid genomes and found that they all show large IAP expansion, with new combinations of protein domains, suggestive of evolutionarily novel aphid-specific functions.

insects | *Acyrthosiphon pisum* | apoptosis | caspases | IAPs

Programmed cell death is essential for the controlled removal of unnecessary, damaged, or potentially dangerous cells. It includes apoptosis and nonapoptotic forms of cell death (1, 2). Apoptosis is the best studied and has roles in development (3), tissue homeostasis (4), and the immune response (5). It involves the activation of several evolutionarily conserved proteases named caspases (cysteinyl aspartate proteinases) (2). All caspases contain a structurally conserved catalytic domain, named "peptidase C14" or "CASc" (6). They are subdivided in initiator and effector caspases based on the size of their prodomain. Their binding to adaptor proteins activates initiator caspases, which can, in turn, activate effector caspases. This leads to the cleavage of cellular substrates and the ordered disassembly of cells, accompanied by typical morphological changes (7). The activity of caspases is controlled by a wide variety of regulators, including pro- and antiapoptotic proteins, inhibitors of apoptosis (IAPs) and IAP-antagonists (8, 9). IAPs directly bind and inhibit activated caspases via an evolutionary conserved Baculovirus IAP-Repeat (BIR) domain (8, 9). Some IAPs also contain a Really Interesting New Gene (RING) zinc finger domain that can either promote or block apoptosis depending on the physiological state of the cell.

The molecular mechanisms of apoptosis have been studied extensively in *Caenorhabditis elegans*, *Drosophila melanogaster*, mice, and humans. In all cases, the same categories of proteins (adaptor proteins, initiator caspases, effector caspases, and regulatory proteins) are present, but their numbers and specific functions can vary widely (2, 8, 10). It has been proposed that the number of apoptosis-associated proteins is correlated with increased organismal complexity and the accompanying functional redundancy and cell type–specific functions (2). However, this remains largely untested. Among insects, which represent the most speciose group of animals, the fruit fly *D. melanogaster* remains the only species in which apoptosis has been extensively studied (10, 11). The *Drosophila* genome encodes one adaptor protein (Ark), three initiator caspases (Dronc, Dredd, and Strica), four effector caspases (DrICE, Dcp-1, Damm, and Decay), and four IAPs (DIAP1, DIAP2, dBruce, and Deterin). Dronc and DrICE are the main caspases of *D. melanogaster* and

Significance

Apoptotic processes play an important role in the development and physiology of almost all metazoan clades. In the highly diverse group of insects, apoptotic pathways have been characterized in only a few dipteran and lepidopteran species, which may not be representative of all insect species. Here, we report the first complete annotation of the apoptotic pathway in a hemipteran insect, the pea aphid *Acyrthosiphon pisum*. We showed that its apoptotic pathway is rewired compared to other insects, with a significant increase in the number of inhibitors of apoptosis (IAPs) and evidence for functional diversification and structural modularity of this protein family. These novelties are widespread in the aphid lineage, suggesting a yet not understood novel aphid-specific function of IAPs.

Author contributions: M.R.L., N.P., P.C., and F.C. designed research; M.R.L., K.G., C.H., G.D., J.O., P.B., E.J., P.D.S., and K.H. performed research; M.R.L., N.P., K.G., S.P., H.C., E.J., P.D.S., K.H., P.C., and F.C. analyzed data; and M.R.L., P.C., and F.C. wrote the paper.

The authors declare no competing interest.

This article is a PNAS Direct Submission.

[1]To whom correspondence may be addressed. Email: patrick.callaerts@kuleuven.be or federica.calevro@insa-lyon.fr.

This article contains supporting information online at https://www.pnas.org/lookup/suppl/doi:10.1073/pnas.2013847117/-/DCSupplemental.

First published December 7, 2020.

are involved in almost all developmental apoptotic processes (11). Dronc is constitutively activated in most *Drosophila* cells, and cell viability is guaranteed by the antiapoptotic action of DIAP1. Cell death happens only when DIAP1 is destabilized through binding of IAP antagonists that hinder the interaction with activated caspases and promote DIAP1 autoubiquitination (11, 12). Aside from *Drosophila*, apoptosis proteins have been studied in a few other dipteran and some lepidopteran species (13–21). These studies found important differences in gene numbers and in the regulation of apoptosis (10, 14, 22–24). Thus, even though the information gathered for *Drosophila* has been essential in advancing our understanding of apoptosis, it seems unlikely that the results can be generalized to all insects.

Aphids are hemimetabolous insects belonging to the Hemiptera, an earlier-diverging and distantly related order compared to the holometabolous Diptera and Lepidoptera (25). Aphids are economically important pests of agriculture and forest crops. They have an evolutionary ancient (150 to 180 million years old) obligate symbiotic relationship with the gamma proteobacterium *Buchnera aphidicola* (26) and show extensive polyphenisms, including parthenogenetic and sexual reproduction and the presence of winged and nonwinged morphs (27, 28). Limited information is available concerning programmed cell death in aphids. Earlier studies indicate that the selective degeneration of flight muscles of winged morphs is apoptosis-related (29). A stress-induced form of apoptosis was also reported for the gut upon feeding toxic compounds to different aphid species (30). Finally, a new form of cell death, involved in the elimination of bacteriocytes, the cells harboring symbiotic bacteria, has been found in senescent pea aphids (31). The distant phylogenetic position of aphids relative to Diptera and Lepidoptera, the presence of different and cell-type–specific forms of cell death, and the fact that eleven aphid genomes have been sequenced to date (28), make aphids an excellent study-system for the investigation of apoptotic pathway diversity in insects.

In the present study, we used a newly improved version of the genome of the pea aphid *Acyrthosiphon pisum* (32), phylogenetic analyses, and protein domain identification to fully annotate the apoptotic pathway in this insect. We found that the proapoptotic part of the pathway comprises homologs for four of the seven *D. melanogaster* caspases. The inhibitory part underwent an extensive expansion, with 28 IAPs, far more than the four to seven found in other insect species (11, 16, 33). Based on their homology to *D. melanogaster* IAP sequences and structures, we selected seven *A. pisum* IAP genes for further studies. We demonstrated that five out of seven are specifically induced throughout bacteriocyte cell death. Structural modeling revealed that the corresponding proteins contain motifs essential to inhibit caspases. Heterologous expression in fruit fly eyes demonstrated the ability of those five selected IAPs to inhibit apoptosis in vivo. Interestingly, *A. pisum* IAPs with the strongest antiapoptotic activity have two RING domains, a feature not observed in any other organisms. Finally, we found that all aphids exhibit an IAP expansion with novel combinations of protein domains, which is suggestive of functional diversification and the emergence of aphid-specific functions.

Results

The Proapoptotic Part of the Apoptotic Pathway in *A. pisum*. Protein sequences from *D. melanogaster* were used to annotate the apoptotic pathway of the pea aphid. Homology relationships between aphid and other previously characterized insect caspases were further elucidated by phylogenetic reconstruction (Fig. 1*A* and *SI Appendix*, Fig. S1). To facilitate their identification, pea aphid caspases were named by combining the prefix Ap-, for *A. pisum*, with the name of their closest homolog in *D. melanogaster*, and paralogs were numbered to differentiate between them (*SI Appendix*, Table S1). We identified a single gene encoding the adaptor protein Ap-Ark and six genes encoding putative caspases in the pea aphid genome (Fig. 1*B*). Based on the phylogenetic reconstruction, the six caspases can be divided in three groups of two paralogs each, more closely related to each other than to any other sequences, revealing a diversification in the aphid branch (Fig. 1 *A* and *B*). Caspases from group I are clear homologs of *Drosophila* Dronc. Caspases from group II and group III showed the highest amino acid percentage identity with the closely related *D. melanogaster* effector caspases DrICE and Dcp-1, with values ranging from 42 to 59% (Dataset S1). The phylogenetic reconstruction confirmed that Ap-ICE-1 and Ap-ICE-2 are indeed closely related to *Drosophila* caspases DrICE and Dcp-1. The homology of Ap-Decay-1 and Ap-Decay-2 with *D. melanogaster* Decay was further confirmed using OrthoDB version 10.1 (34). Several transcripts are predicted for most of the pea aphid caspases (*SI Appendix*, Table S1), while in *D. melanogaster*, single transcripts have been identified for each of their homologs. No pea aphid homolog for the caspases Dredd, Strica, and Damm was found.

A. pisum Caspases Are Expressed and Contain the Functional Domains Needed to Promote Apoptosis. To determine whether pea aphid putative caspases are functional, we analyzed 1) their expression in whole insects, 2) their domain composition, and 3) the presence of residues critical for enzymatic function (Fig. 1 and *SI Appendix*, Fig. S2).

RT-PCR assays on complementary DNA (cDNA) prepared from pooled whole aphids, spanning the entire nymphal (N1, N2, N3, and N4) and adult (A9, A15, and A23) stages of the aphid life cycle, revealed that the genes encoding the putative Ap-Ark and caspases are all expressed (Fig. 1*C*). It was not possible to investigate *Ap-decay-1* and *Ap-decay-2* independently given their strong similarity, which prevented the design of paralog-specific primers.

All CASc domains of *A. pisum* putative caspases are composed of the two subunits found in other organisms (p20 and p10), separated by an intersubunit linker (Fig. 1*B*). Group I caspases (Ap-Dronc-1 and Ap-Dronc-2) have long prodomains (>130 amino acids), while group II caspases (Ap-ICE-1 and Ap-ICE-2) have short prodomains (<80 amino acids) (Fig. 1*B*), suggesting roles as initiator and effector caspases, respectively. Ap-Dronc-1 and Ap-Dronc-2 prodomains also contain a Caspase Recruitment Domain (CARD) (Fig. 1*B*), which confirms their homology with *D. melanogaster* Dronc. It is not clear whether *A. pisum* group III caspases act as initiator or effector caspases; Ap-Decay-1 has a long prodomain of more than 170 amino acids, not harboring any specific domain, whereas Ap-Decay-2 has no prodomain.

Comparative sequence analysis revealed that all putative pea aphid caspases have the universally conserved Q-A-C-[RQG]-[GN] sequence in the p20 subunit of their CASc domain, with the catalytic cysteine found in the core active site of most caspases (6) (*SI Appendix*, Fig. S2). The only exception is Ap-Dronc-1, which contains a unique D-A-C-R-G motif. This is a common feature of Dronc-like proteins, which have specific motifs: P-F-C-R-G in *D. melanogaster* (13), S-I-C-R-G in *Aedes aegypti* (13), and Q-M-C-R-G in *Spodoptera frugiperda* (15). These caspases are all enzymatically active. In *Drosophila*, the replacement of the first glutamine by a proline allows Dronc to cleave proteins after aspartate or glutamate residues (35). In *A. pisum*, the replacement of a neutral amino acid with a negatively charged one could have important consequences for the specificity of this protein and its functions. Other key residues for catalysis and substrate recognition include the conserved arginine, histidine, and glycine residues in the p20 subunit upstream of the core active site and another conserved arginine in the p10 subunit (6). Those four residues are conserved in all pea aphid caspases (at positions 28, 85, 86, and 175, respectively) with the exception of Ap-Dronc-1, where the first arginine has been

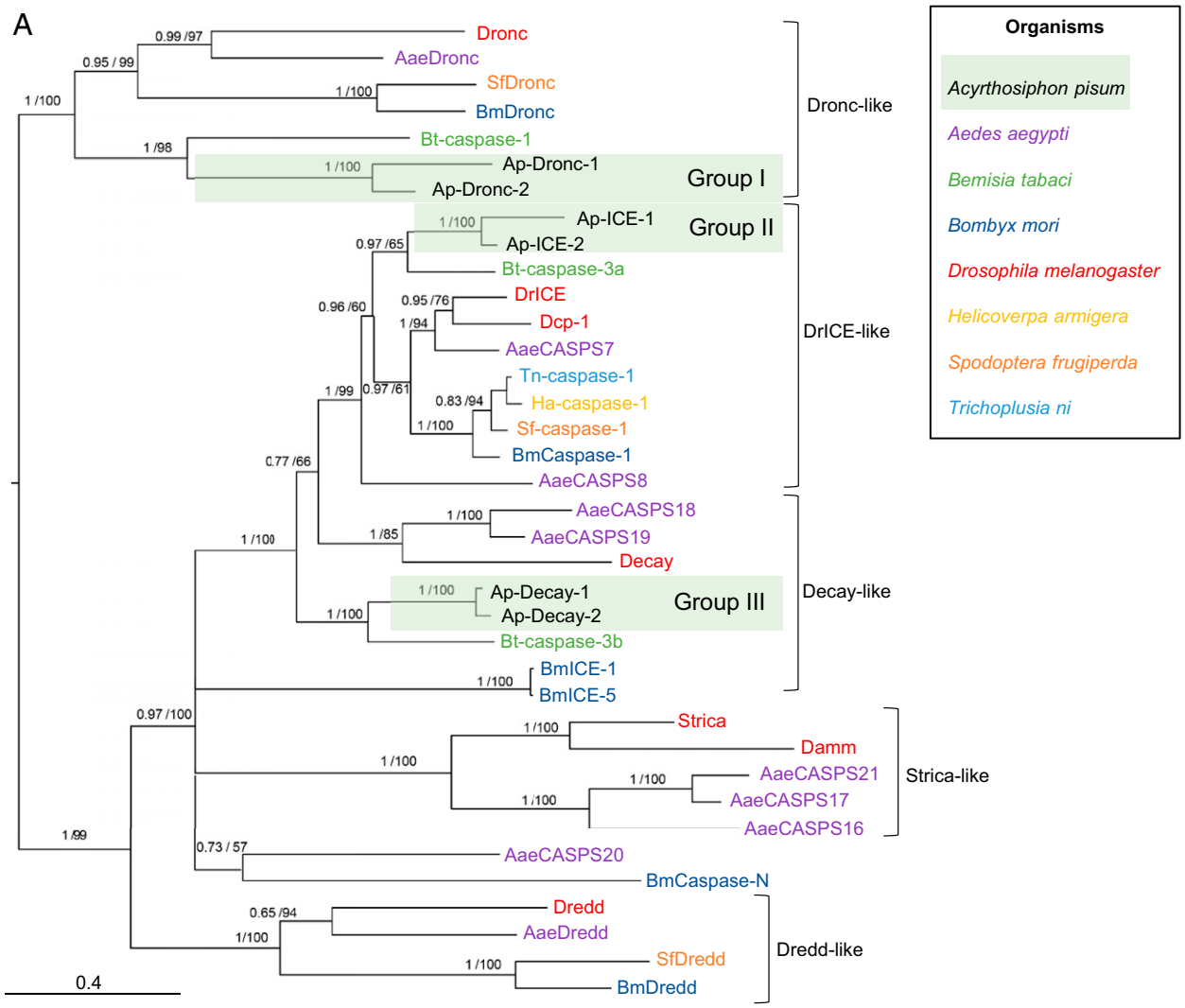

Fig. 1. Identification of caspase- and adaptor protein-encoding genes in the pea aphid genome. (*A*) The phylogenetic relationships between caspase protein sequences found in *Acyrthosiphon pisum* and a selection of insect species based on CASc domain alignment. For each node, Bayesian posterior probability and bootstrap values are indicated. A group of putative *A. pisum* caspase paralogs are also indicated. Midpoint rooting was used to present the tree. (*B*) The domain architecture of the pea aphid putative caspases and adaptor proteins. Each caspase possesses a CASc domain (CASpase catalytic domain) composed of two distinct subunits (p20 and p10) and preceded by a prodomain of variable size. Ap-Dronc-1 and Ap-Dronc-2 possess an additional CARD domain (Caspase Recruitment Domain) at their N terminus. The putative adaptor protein Ap-Ark contains a CARD domain, a NB-ARC domain, and multiple WD40 repeats. The position of amino acids that mark the beginning and the end of the different domains are indicated below each structure. (*C*) Pea aphid putative caspases and adaptor proteins genes are expressed. The sequences were successfully amplified from a pool of cDNA obtained from whole aphids at different life stages. For each primer set, a negative control was performed on samples devoid of cDNA. MW, molecular weight marker.

replaced by an isoleucine. This is unusual and has not been found in other Dronc-like proteins. Finally, to be activated, effector caspases need to be cleaved by initiator caspases at a conserved aspartate residue present in their intersubunit linker. Ap-ICE-1, Ap-ICE-2, Ap-Decay-1, and Ap-Decay-2 all possess the conserved aspartate residue at position 146 that is also present in *Drosophila* DrICE. This indicates that those caspases have the potential to be cleaved and thus activated. This conserved aspartate is not present in *Drosophila* Dronc and its pea aphid homologs, which is consistent with cleavage not being necessary for Dronc activation (35).

The *A. pisum* Genome Has an Expanded IAP Repertoire. Next, we used the four *D. melanogaster* IAP sequences to identify putative homologs encoded in the pea aphid genome. A total of 33 proteins, corresponding to 28 genes, were identified as IAPs (containing at least one BIR domain) (*SI Appendix*, Table S1). Other eukaryotic species in which IAPs have been systematically investigated usually have fewer than 10 IAPs (e.g., four in the mosquito *Aedes aegypti* (33) and the silkworm *Bombyx mori* (16), eight in humans (8), and two in *Caenorhabditis elegans* (36)). Thus, the inhibitory part of the pea aphid apoptotic pathway seems to have expanded extensively.

Phylogenetic reconstructions, based on the alignments of their BIR domains, allowed us to sort the pea aphid IAPs into four groups of paralogs more closely related to each other than to any other sequences (Fig. 2*A* and *SI Appendix*, Fig. S3). The first group includes two Deterin homologs, Ap-Deterin-1 and Ap-Deterin-2 (Fig. 2*B*). The remaining three groups contain BIR domains more closely related to the ones found in DIAP-like proteins than in Deterin-like proteins. These IAPs were given a name composed of the prefix Ap-, for *A. pisum*, followed by IAP and a letter (A, B, or C) relative to their paralogy group. The different paralogs were further numbered to distinguish them. The A, B, and C paralog groups comprise 4 (Ap-IAP-A1 to -4), 1 (Ap-IAP-B1), or 21 (Ap-IAP-C1 to -21) proteins, respectively. Despite being homologs of DIAP1 and DIAP2, proteins from those three groups exhibit different domain architectures. Ap-IAP-A1 to -4 possess two BIR domains, like DIAP1, but have two RING domains instead of one (Fig. 2*B*). Importantly, they are the only known IAPs to date with more than one RING domain (*SI Appendix*, Fig. S4). Ap-IAP-B1 has one RING domain and one UBA domain, like DIAP2, but two BIR domains instead of three. While their numbers vary, the presence in Ap-IAP-A and -B of BIR and RING domains that are also present in DIAP1 and DIAP2 suggests a common function. Inversely, Ap-IAP-C1 to -21 possess a unique BIR domain and are notably shorter (*SI Appendix*, Table S1). Based on the phylogeny, proteins from group C seem to be the result of an extensive aphid-specific expansion. Since proteins from this group lack a RING domain, it seems unlikely that they function similarly to DIAP1 and DIAP2 despite being homologs of those two proteins. The fact that so many duplicates of Ap-IAP-C are maintained in the pea aphid genome is indicative of their importance in aphid physiology and suggests that they may have acquired new functions and/or have important but yet unidentified roles in apoptotic processes. The hypothesis that a possible functional diversification of Ap-IAP-C took place even inside this group is supported by the analysis of their sequences: some members of Ap-IAP-C are highly divergent (Dataset S2). In contrast to the apparent expansion of its IAP repertoire, the pea aphid genome appears to lack dBruce homologs. This further underlines the unique character of the *A. pisum* apoptotic pathway, as orthologs of dBruce are found in many eukaryotic species where IAPs have been systematically searched, apart from yeasts and nematodes (10, 36) (*SI Appendix*, Fig. S4).

***Ap-iap* Expression Varies in a Time- and Tissue-Dependent Manner.** Among the 28 putative IAP-encoding genes of *A. pisum*, we selected group A and B IAPs as well as *Ap-deterin-1* and *-2* for further studies based on their clear homology to *Drosophila* proteins or similar domain composition. RT-PCR conducted on a cDNA pool prepared from whole aphids collected at different life stages revealed that the seven selected IAPs are expressed (Fig. 2*C*).

qRT-PCR experiments allowed us to measure the expression of those seven genes in five different tissues (bacteriocytes, gut, embryonic chains, head, and carcass) and in a selected number of life stages (Fig. 3 and *SI Appendix*, Fig. S5). All genes presented widely diverging spatiotemporal expression patterns with none being expressed exclusively in one tissue or at one stage. *Ap-iap-A1* and *-B1* are highly expressed in all tissues and stages, suggesting that they may play a major role in aphid physiology (Fig. 3*A*). *Ap-iap-A2*, *Ap-iap-A4*, and *Ap-deterin-1* have low to medium expression levels in all tissues and life stages. They could act redundantly, or in synergy, with *Ap-iap-A1* and *-B1*. Although *Ap-iap-A3* is weakly expressed in whole aphids (Fig. 2*C*), we could not find evidence of *Ap-iap-A3* expression in any of the tissues or stages analyzed. An explanation for this is that this gene is expressed at such low levels that it fails to reach our detection threshold when considering isolated tissues. Alternatively, *Ap-iap-A3* may be expressed in tissues, developmental stages, or conditions that were not tested here. *Ap-deterin-2* was the only gene with a more restricted, low-level expression in the head, carcass, and embryonic chains.

Overall, five (*Ap-iap-A1*, *Ap-iap-A2*, *Ap-iap-A4*, *Ap-iap-B1*, and *Ap-deterin-1*) of the seven tested IAPs are expressed in the bacteriocytes. Interestingly, these five genes are also specifically induced in adult bacteriocytes (Fig. 3*B* and *SI Appendix*, Fig. S5), at stages corresponding to the onset of the novel type of cell death recently described in bacteriocytes (31). *Ap-deterin-1* and *Ap-iap-A4* are progressively induced in bacteriocytes only. *Ap-iap-A1*, *-A2*, and *-B1* are also induced in the gut and the carcass in late stages. However, this induction remains distinct from the one observed in bacteriocytes, as it can either start earlier (e.g., *Ap-iap-A1* in the carcass) or later (e.g., *Ap-iap-B1* in the carcass) or be transient (e.g., *Ap-iap-A1* and *-A2* in the gut) or biphasic (e.g., *Ap-iap-A2* and *-B1* in the carcass).

Ap-IAPs Are Potentially Antiapoptotic. To identify their antiapoptotic potential, we compared the BIR domain sequences of the five IAPs that are induced in aphid bacteriocyte cell death with those of *D. melanogaster* IAPs. The two BIR domains of Ap-IAP-A1, -A2, -A4, and -B1 contain the three cysteines and one histidine, organized in the C-X_2-C-X_{16}-H-X_6-C motif, that are responsible for the formation of the Zn^{2+} ion chelating fold of BIR domains (8) (Fig. 4*A*). Nevertheless, several other residues that have been reported as being important for the correct conformation of the chelating fold and caspase binding are not conserved in *A. pisum* BIR domains (37, 38). Ap-Deterin-1 has a unique BIR domain, where the histidine and third cysteine of the Zn^{2+} binding motif are separated by 10 amino acids instead of 6. Even though Deterin-like proteins are known to have longer BIR domains, the additional residues are usually found upstream of the first zinc-binding cysteine residue and not in the middle of the motif. Importantly, despite a domain composition similar to Deterin-like proteins, members of the Ap-IAP-C group do not have additional residues or long BIR domains. This, coupled with the observation that the BIR domain of these proteins is closely related to the ones found in DIAP-like proteins (Fig. 3*A*), strengthens the notion that proteins of this group do not represent an expansion of aphid Deterin-like proteins.

To assess if this specific organization could alter the Zn^{2+} chelating fold and prevent binding of caspases, we generated three-dimensional (3D) structure models of the BIR domains for

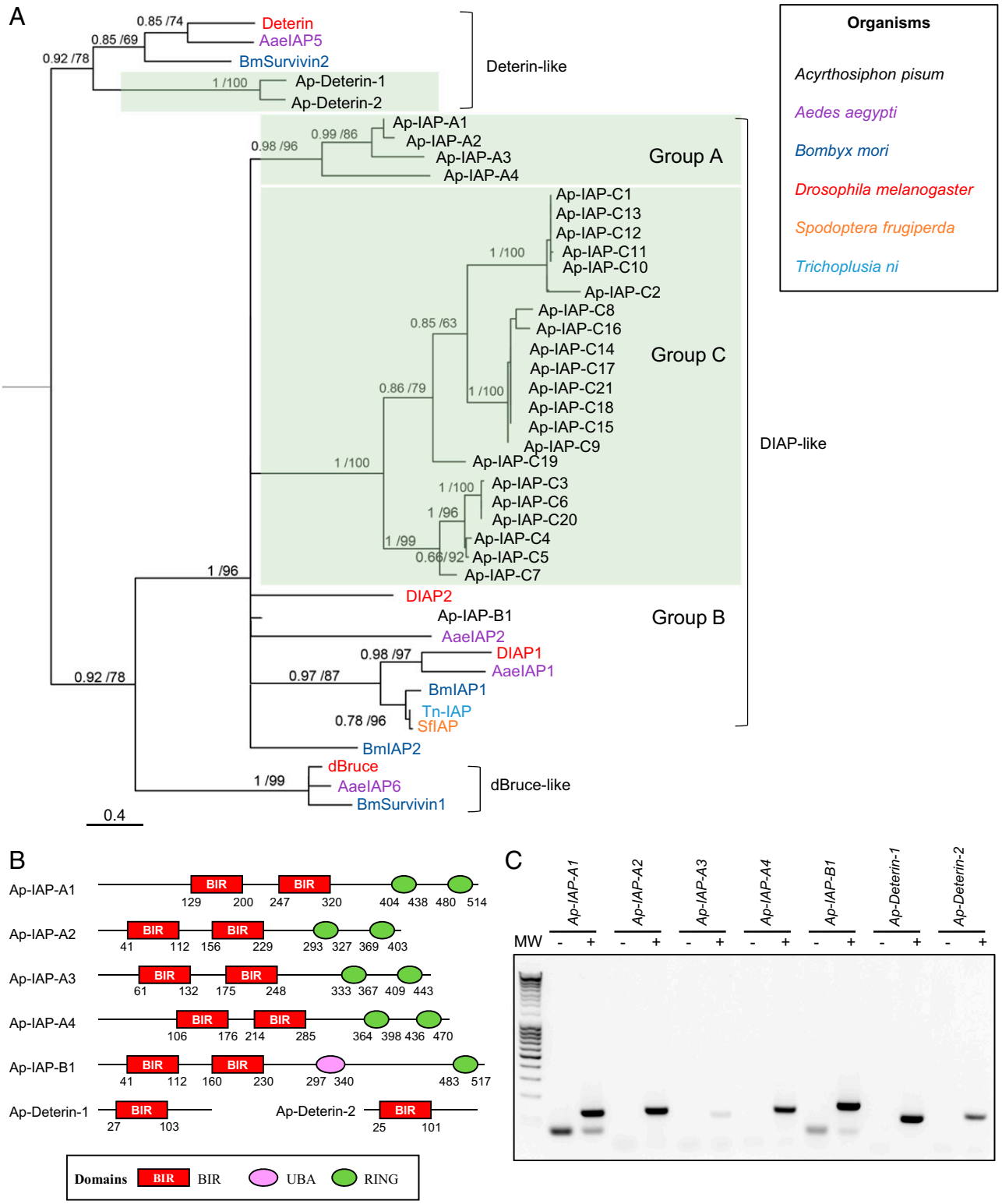

Fig. 2. Identification of IAP-encoding genes in the pea aphid genome. (*A*) The phylogenetic relationships between IAP protein sequences found in *Acyrthosiphon pisum* and a selection of insect species based on BIR domain alignment. For each node, Bayesian posterior probability and bootstrap values are indicated. A group of putative *A. pisum* IAP paralogs are also indicated. This tree was generated using one representative BIR domain from each IAP sequence (full procedure described in the *SI Appendix, Supplementary Materials and Methods*). Midpoint rooting was used to present the tree. (*B*) The domain architecture of selected pea aphid putative IAPs. Each IAP contains at least one BIR domain (Baculoviral IAP Repeat). Additional domains include UBA (ubiquitin-associated domain) and/or RING domains. The positions of amino acids that mark the beginning and the end of the different domains are indicated below each structure. (*C*) Pea aphid putative IAP genes are expressed. The sequences were successfully amplified from a pool of cDNA obtained from whole aphids at different life stages. For each primer set, a negative control was performed on samples devoid of cDNA. MW, molecular weight marker.

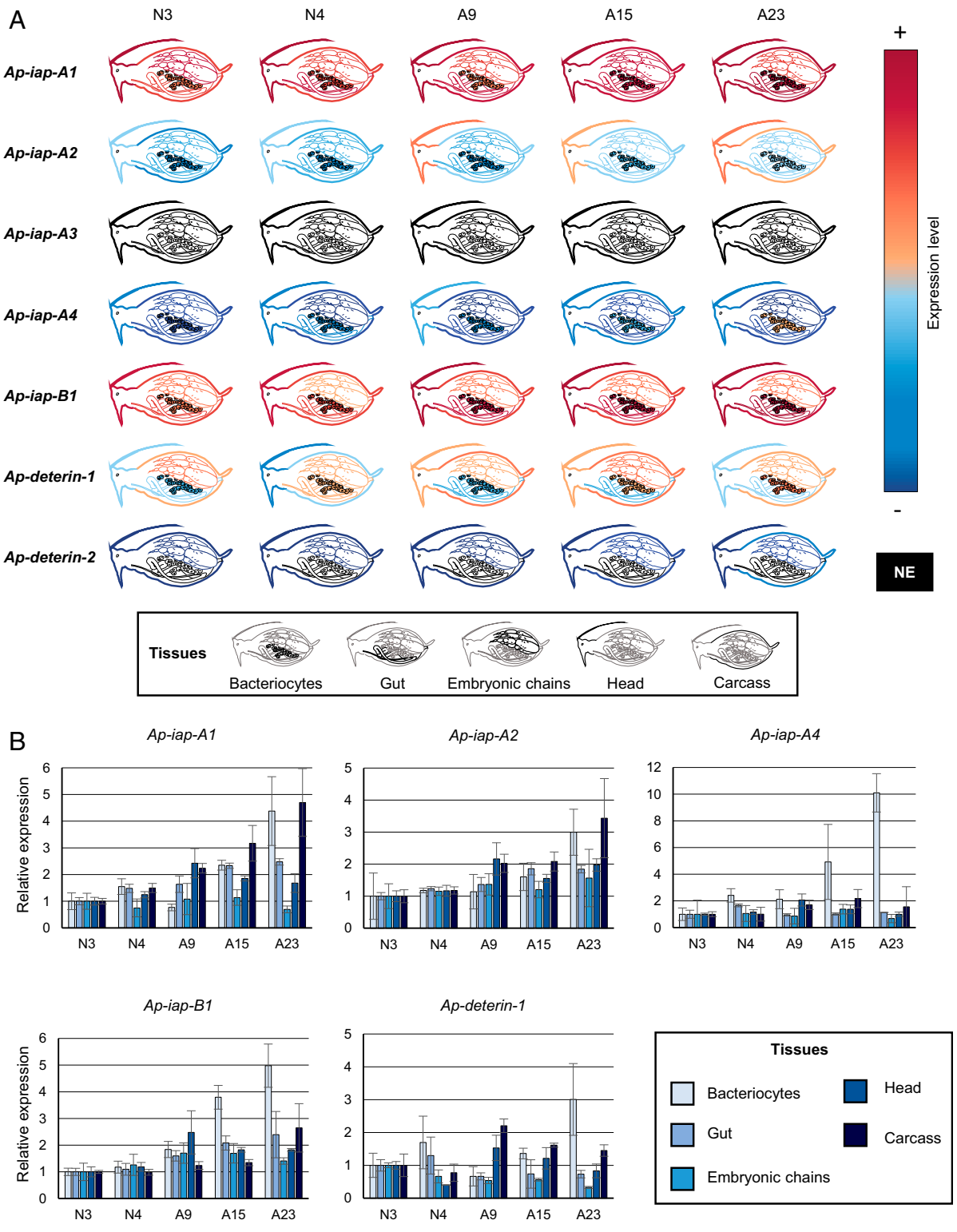

Fig. 3. The expression patterns of pea aphid *iap* mRNAs across tissues and time. (*A*) The expression levels of seven selected pea aphid IAPs in different tissues at selected developmental times based on qRT-PCR data analysis. The levels of expression are illustrated by a color scale, going from red (highly expressed) to blue (lowly expressed). Tissues in which the gene is not expressed at a particular time point are represented in black. The expression levels were normalized relatively to the *rpl7* gene. (*B*) The expression levels of selected pea aphid IAPs in different tissues throughout aphid development based on qRT-PCR data analysis. *iap* mRNA gene-expression levels in the different tissues are expressed relative to N3 levels. Data are presented as means ± SD from three independent biological replicates. mRNA, messenger RNA; NE, not expressed.

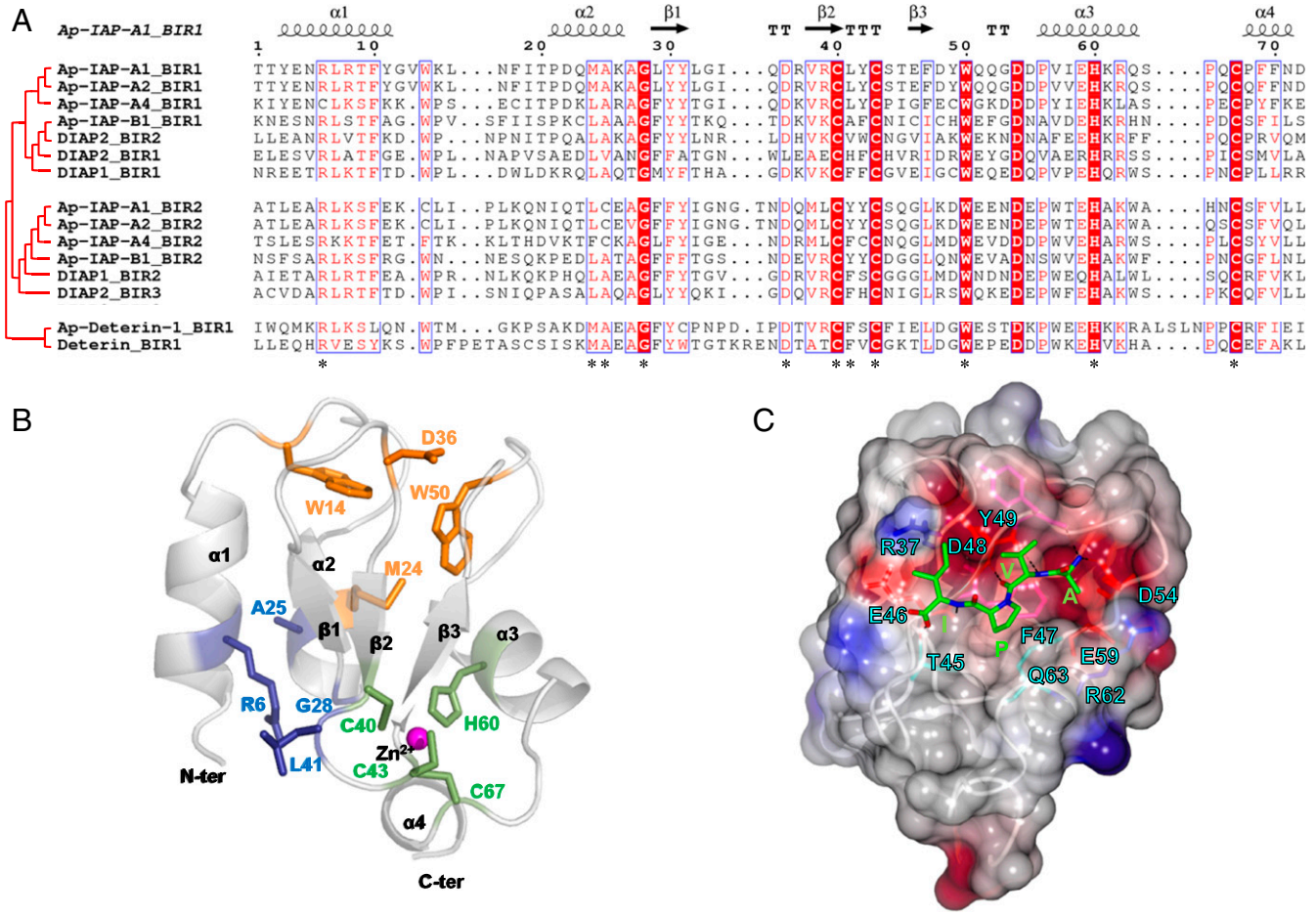

Fig. 4. The sequence alignment, 3D modeling, and secondary structure reconstruction of BIR domains in pea aphid IAPs. (*A*) The sequence alignment of BIR domains from selected *Acyrthosiphon pisum* and *Drosophila melanogaster IAP* shows conserved motifs (highlighted in red when fully conserved, written in red when partially conserved). The residues involved in the correct conformation of the Zinc chelating fold are indicated by an asterisk. The corresponding secondary structure (arrow, β-strand; helix, α-helix) is reported in black above the alignment (Ap-IAP-A1_BIR1 domain as a reference). (*B*) A 3D-modeled structure prediction of the Ap-IAP-A1_BIR1 domain with a focus on the three structural padlocks (highlighted in green, blue, and orange) stabilizing the BIR-specific zinc-chelating fold (magenta). (*C*) The structural features of the predicted IBM groove of the Ap-IAP-A1_BIR1 domain binding the tetrapeptide AVPI (green stick). The electrostatic surface of Ap-IAP-A1_BIR1 domain is represented with the negatively and positively charged regions (red and blue, respectively). Only the residues interacting with AVPI are represented as colored sticks and labeled. The hydrogen bonds anchoring the tetrapeptide AVPI in the IBM groove are represented as black dashes.

Ap-IAP-A1, -B1, and Ap-Deterin-1. Our models predict that, like BIR domains from other organisms (8, 37, 38), each aphid IAP BIR domain comprises a Zn^{2+} chelating fold composed of a central antiparallel three-β-stranded-sheet (β1-3), surrounded by four α-helices (α1-4). This fold is stabilized by the presence of three "lock regions" that mostly involve hydrogen bonds and hydrophobic interactions (Fig. 4*B* and *SI Appendix*, Fig. S6 *A* and *B*). Our modeling results also predict that the additional residues present in Ap-Deterin-1 have no impact on the conformation of its chelating fold (*SI Appendix*, Fig. S6*A*).

3D structure predictions suggest that the tested *A. pisum* BIR domains contain the IBM (IAP binding motif)-binding groove, a cleft surface involved in the binding of caspases and IAP antagonists that is conserved in *D. melanogaster* and human BIR domains (37, 38). As in BIR domains from other organisms, the predicted binding groove in *A. pisum* IAP BIR domains is located between the α_3 helix and β_3 strand (Fig. 4*B*). Its ability to accommodate the AVPI tetrapeptide present in the IAP-antagonist Smac suggests that it has the potential to bind IAP antagonists and caspases (9). Consistent with this, we predicted multiple specific bonds that may stabilize the interaction between the binding groove and the AVPI tetrapeptide (Fig. 4*C*). Notably, none of the pea aphid BIR domains has an acidic residue at the position preceding the histidine, a configuration that has been predicted to prevent the binding of caspases in BIR domains from other organisms (37).

Ap-IAPs Are Able to Inhibit Apoptosis In Vivo. Sequence analyses, secondary structure prediction, and 3D modeling all confirmed that the BIR domains of bacteriocyte-expressed IAPs have the potential to bind caspases. However, in the literature, there are examples of IAPs that are able to bind caspases yet have a very low antiapoptotic potential (39). Furthermore, the five IAPs tested here have different domain combinations (only one BIR domain for Ap-Deterin-1, two BIR and one RING for Ap-IAP-B1, and two BIR and two RING domains for Ap-IAP-A1, -A2, and -A4), which could have an effect on their ability to inhibit apoptosis. Due to the difficulty of systematically inactivating highly identical genes (40) and the limits of the RNA interference (RNAi) technology in aphids (41), we decided to assess the antiapoptotic ability of the pea aphid IAPs using a tractable in vivo model, the *D. melanogaster* developing eye. *Ap-IAPs* were expressed using the well-characterized GAL4-UAS system (42). In the transgenic *D. melanogaster* lines used for this experiment,

the GAL4-coding sequence is located downstream of eye-specific glass multiple reporter (GMR) regulatory sequences that also drive the constitutive expression of the proapoptotic gene *rpr*. The resulting flies undergo massive apoptosis in the eyes, leading to a characteristic small-eye phenotype (Fig. 5 *A*–*F* and *SI Appendix*, Fig. S7*A*). Expression of a functional antiapoptotic IAP in the eye is able to reverse the effect of *rpr* and restore the wild-type phenotype (43).

In this work, we used this assay, for the first time, to study *A. pisum* genes. Two to three transgenic lines for each of the five selected IAPs (Fig. 5 and *SI Appendix*, Fig. S7) were generated. Similar to what we observed for *Drosophila diap1* (used as a positive control for rescue of the eye phenotype), the GMR-*rpr*–dependent small-eye phenotype was nearly completely suppressed by the expression of *Ap-iap-A1* (Fig. 5*B*), *Ap-iap-A2* (Fig. 5*C*), or *Ap-iap-A4* (Fig. 5*D*). The expression of *Ap-iap-B1* (Fig. 5*E*) and *Ap-deterin-1* (Fig. 5*F*) only weakly suppressed this phenotype. To quantify the antiapoptotic potential and compare the relative strength of each IAP, we measured the eye surface/head surface ratio in control (only the gene *rpr* is expressed) and rescue (coexpression of *rpr* with a pea aphid *iap* gene) flies from the different transgenic lines. We found a prominent increase in eye surface/head surface ratio for the genes *Ap-iap-A1*, *Ap-iap-A2*, and *Ap-iap-A4*, confirming that these IAPs have stronger antiapoptotic potential. Interestingly, while Ap-IAP-B1 and Ap-deterin-1 have one or no RING domain, the structure of Ap-IAP-A1, -A2, and -A4 comprises two RING domains. Based on these in vivo experiments, we propose that the presence of two RING domains conveys a greater antiapoptotic potential to pea aphid IAPs.

Aphid IAPs Present Undocumented Domain Association Patterns. We finally extended our annotation and analysis of the apoptotic pathways to all of the aphid genomes available on the National Center for Biotechnology Information (NCBI) or made available on the AphidBase (44) website prior to publication (Table 1). *Daktulosphaira vitifoliae*, a major historic pest of viticulture belonging to the sister family of Aphididae (i.e., Phylloxeridae family), was also analyzed (45). Notably, all those species have fewer caspases than *D. melanogaster*, but they possess at least one putative initiator caspase and one putative effector caspase, with the exception of *Aphis gossypii* and *Rhopalosiphum padi*, for which only caspases with long prodomains have been identified (*SI Appendix*, Table S2). We also found that aphids consistently have a greater number of IAPs (*SI Appendix*, Table S3) than *D. melanogaster*, but the numbers vary between species without correlation between these numbers and with the genome size or the number of protein-coding genes (Table 1 and *SI Appendix*, Table S3). Aphid IAPs can be grouped in 14 classes based on domain patterns (Fig. 6 and *SI Appendix*, Table S3). These structures are either found in all aphids, in a subset of aphids, or in a single species. Overall, aphid IAPs have between one and five BIR domains and between one and three RING domains, while IAPs from other organisms have, at most, three BIR domains and one RING domain (*SI Appendix*,

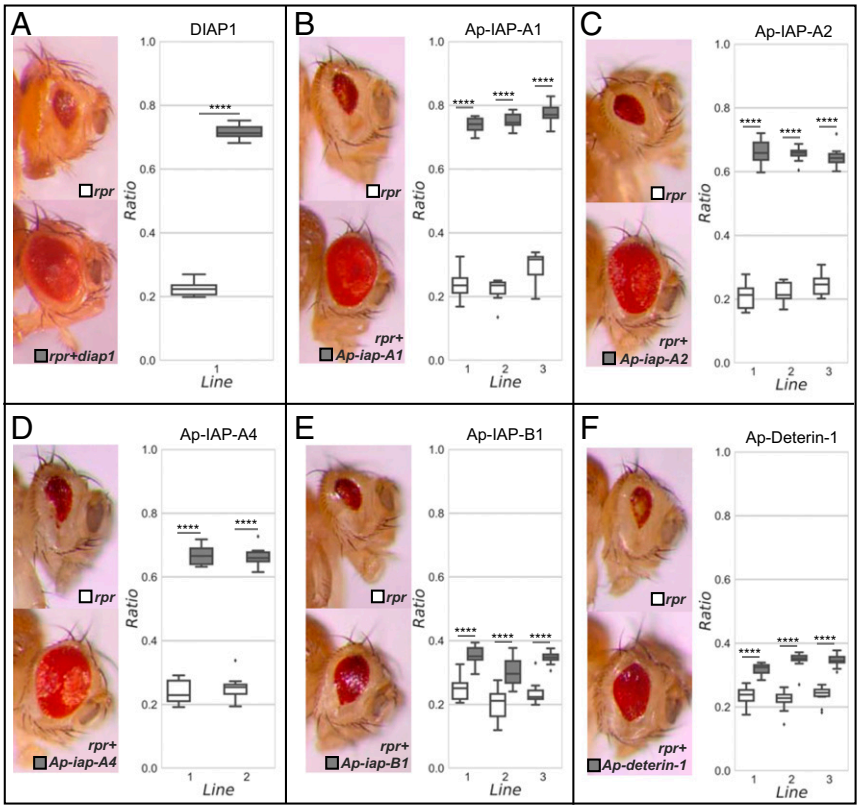

Fig. 5. The antiapoptotic potential of pea aphid IAPs assessed in *Drosophila* eyes. Five pea aphid IAP genes (*Ap-iap-A1*, *Ap-iap-A2*, *Ap-iap-A4*, *Ap-iap-B1*, and *Ap-deterin-1*) were targeted to the eye to measure the level of suppression of *rpr*-induced apoptosis. Near complete suppression of apoptosis is seen upon coexpression with *diap1* (*A*), *Ap-iap-A1* (*B*), *Ap-iap-A2* (C), and *Ap-iap-A4* (*D*). The coexpression of *Ap-iap-B1* (*E*) and *Ap-deterin-1* (*F*) only partially rescued this phenotype. A comparison of eye surface/head surface ratio in control (white; only the gene *rpr* is expressed) and rescue (gray; the gene *rpr* is coexpressed with a pea aphid *iap* gene) flies from the different transgenic lines confirmed those results. The coexpression of an *Acyrthosiphon pisum iap* with *rpr* systematically led to a significant increase in eye surface/head surface ratio due to an increase in eye size. This increase was more prominent for the genes *Ap-iap-A1*, *Ap-iap-A2*, and *Ap-iap-A4,* with a ratio similar to what was observed for *diap1*. The pea aphid IAPs with the strongest antiapoptotic potential are the ones containing two RING domains. The statistical significance was evaluated using the two-sided Mann–Whitney *U* test; ****$P < 0.0001$.

Table 1. Variation in the number of apoptosis-related genes in the aphid lineage

Species	Caspases	IAPs	Genome size (Mbp)	Genes encoding proteins	Assembly	Annotation release
*Acyrthosiphon. pisum**	6	28	541	18277	GCA_005508785.1	Annotation release 103
Aphis glycines[†]	4	26	303	42247	Assembly v1.0	Annotation v1.0
*Aphis gossypii**	3	10	294	12828	GCA_004010815.1	Annotation release 100
*Cinara cedri**	3	12	396	22234	GCA_902439185.1	Annotation release 100
Daktulosphaira vitifoliae[†]	4	31	283	25814	Assembly 3.1	Annotation v3.2
*Diuraphis noxia**	3	6	397	12377	GCA_001186385.1	Annotation release 100
*Melanaphis sacchari**	3	19	300	12320	GCA_002803265.2	Annotation release 100
Myzus cerasi[†]	5	9	406	28688	Assembly v1.1	Annotation v1.1
*Myzus persicae**	4	21	347	14993	GCA_001856785.1	Annotation release 100
*Rhopalosiphum maidis**	4	12	326	12060	GCA_003676215.3	Annotation release 101
Rhopalosiphum padi[†]	5	20	321	26535	Assembly v1.0	Annotation v2.0
*Sipha flava**	4	10	353	13575	GCA_003268045.1	Annotation release 100

The complete lists of caspase- and IAP-encoding genes are available in the *SI Appendix*, Tables S2 and S3, respectively. Proteins were considered as putative caspases or IAPs if they possess at least one CASc or one BIR domain, respectively.
*Species for which genomic data were obtained from the NCBI database.
[†]Species for which genomic data were obtained from the AphidBase database.

Fig. S4). Importantly, all aphids possess IAPs with two RING domains. Aphids therefore present other previously undocumented domain patterns that could be associated with the emergence of new functions specific to this insect group.

Discussion

We have demonstrated that, in the aphid lineage, the proapoptotic part of the apoptotic pathway is reorganized and contains a smaller number of proteins compared to dipteran and lepidopteran genomes (10). In the *A. pisum* genome, we identified homologs of *D. melanogaster* Ark, Dronc, DrICE, and Decay but none for Dredd, Strica, and Damm. The latter three are also absent in the other aphid genomes we analyzed here and in the genome of the silverleaf whitefly *Bemisia tabaci*, suggesting a feature common to Hemiptera (46). In *A. pisum*, the absence of those proteins is possibly compensated by the apparent duplications that led to the presence of two initiator caspases (Ap-Dronc-1 and Ap-Dronc-2) and four effector caspases (Ap-ICE-1, Ap-ICE-2, Ap-Decay-1, and Ap-Decay-2). The duplicated caspases might act redundantly in specific tissues, or they might have developed new functions, related or not to apoptosis. In the case of Ap-Dronc-1, which has undergone substitutions in several key residues involved in catalysis and substrate recognition, a possibility is that it acts as a decoy molecule. Decoys are enzymatically inactive caspases that have arisen from gene duplication, undergone substitutions in critical amino acids, and acquired the ability to regulate other caspases (24). They have been identified in multiple organisms, including several insects. Contrary to the pea aphid, other aphid genomes do not show duplication for each of their initiator or effector caspases. Nevertheless, the fact

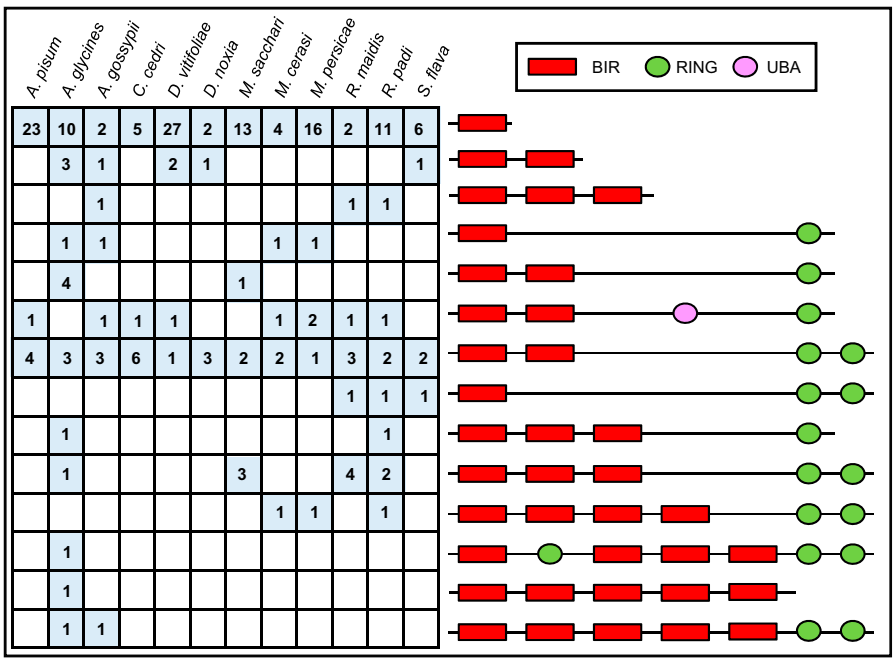

Fig. 6. Aphids possess IAPs with more than three BIR domains and one RING domain. The domain composition of IAP proteins from 11 available aphid genomes and *Daktulosphaira vitifoliae* is shown. The number of protein-encoding genes relative to each IAP domain composition in each species is indicated. Aphid IAPs present an important structural diversity with one to five BIR domains and one to three RING domains. The BIR domains are represented by a red rectangle, the RING domains by a green oval, and the UBA domain by a pink oval. The structures are not represented to scale.

that they all have fewer caspases than *D. melanogaster* may be indicative of how the ancestral form of the pathway was organized. Further studies, including more insect genomes, are needed to infer the ancestral form of the pathway and discriminate between the two possible scenarios: caspases have been lost in a common ancestor of aphids or underwent diversification in Lepidoptera and Diptera orders.

We also found that the inhibitory part of the apoptotic pathway is expanded and shows extensive structural novelty in terms of IAP domain organization. These two features of IAPs seem to be unique to aphids and contrast with what is observed in other insect or arthropod genomes. In addition to lepidoptera and dipteran genomes, we extended our analysis by annotating the IAPs in more ancient insect groups or other arthropods with genomes available in public databases and found that none of them show an expansion of IAPs: four IAPs were found in the genome of the locust *Locusta migratoria* (order: Orthoptera), three in the cockroach *Blattella germanica* (order: Blattodea), five in the honey bee *Apis mellifera* (order: Hymenoptera), and four in *D. melanogaster* (order: Diptera) and in *B. mori* (order: Lepidoptera), ranked from the more ancient to the more recent insect order, following the phylogeny proposed by Misof et al. (25); six IAPs were found in the water flea *Daphnia pulex* (order: Cladocera). A preliminary analysis of their domain composition also shows that none of the arthropod genomes cited above include either novel domain association patterns or more than one RING domain. This analysis provided further support for the notion that both the expansion and the emergence of new domain associations could represent evolutionary innovations of aphid genomes. It also shows that the number of IAPs is not related to the age of the group.

Phylogenetic analyses of the pea aphid IAPs allowed us to identify four groups of paralogs, suggesting that the expansion arose from several aphid-specific duplications. Furthermore, we show that *A. pisum* IAPs are differentially expressed in a tissue- and development-dependent fashion. This is suggestive of functional diversification and specialization that may extend beyond the roles in programmed cell death. Functional specialization of IAPs is also seen in other species (47–50). In *Drosophila*, for example, all IAPs also display functions in nonapoptotic processes. The loss of DIAP1 results in embryonic lethality accompanied by massive apoptosis, but this protein also plays a role in border cell migration in the ovary (48). DIAP2 mostly functions in the immune system following infection by Gram-negative bacteria (49), while mutant alleles for dBruce show defects in spermatogenesis (50).

Here, we consider three possible roles for the aphid IAP expansion.

We previously described a novel type of nonapoptotic cell death for *A. pisum* bacteriocytes, which starts with hypervacuolation of the endoplasmic reticulum and shows an age-associated increase in cellular stress (e.g., reactive oxygen species and endoplasmic reticulum stress) with a concomitant increase of caspase and IAP expression (31). In the present work, we demonstrate that at least five IAPs are expressed in aphid bacteriocytes and are specifically induced during their cell death. We propose that the five bacteriocyte-expressed IAPs were recruited for cell-type specific expression, thus supporting bacteriocyte survival and the continued presence of symbiotic bacteria despite continued high cellular stress in bacteriocytes. Among them, three *A. pisum* IAPs (Ap-IAP-A1, Ap-IAP-A2, and Ap-IAP-A4) have strong antiapoptotic potential in vivo, suggesting that they may play a major role in the inhibition of apoptosis throughout bacteriocyte cell death, with the other two (Ap-IAP-B1 and Ap-Deterin-1) having redundant functions. A possible role in symbiosis is not the only reason for IAP expansion because we also found this expansion in the grape phylloxera *D. vitifoliae*, a nonsymbiotic aphid-related species.

A second possibility we want to consider relates to immunity. Aphids are major vectors of plant pathogenic viruses (51), are readily infected by secondary symbiotic bacteria, and show considerable resistance to bacteria (27). At the same time, aphids have a strongly reduced Immune Deficiency (IMD) pathway, one of the major innate immunity pathways (52). In light of the latter observation, it is tempting to hypothesize that IAPs have an active role in aphid immunity. A link between IAP expansion and immunity has been proposed for other invertebrates, such as the molluscs *Lottia gigantea* (53), *Crassostrea gigas* (54), and *Biomphalaria glabrata* (53). Other Hemiptera, such as psyllids, whiteflies, planthoppers, and leafhoppers, are also important vectors of plant pathogenic viruses, display long-lasting mandatory and facultative relationships with bacterial symbionts, and lack several effectors of the IMD pathway (52). We looked for apoptosis-related proteins in the different hemipteran genomes available, and we found that none of them have an amplification of the IAP family comparable to what we observed in *A. pisum* (three IAPs in *Cimex lectularius* and *Rhodnius prolixus,* four in *B. tabaci*, seven in *Diaphorina citri*, and 14 in *Nilaparvata lugens*). Therefore, even though a role of IAPs in immunity remains a possibility, it seems unlikely to be the only explanation.

Aphids display remarkable polyphenisms, as manifested in parthenogenetic and sexual reproduction and the presence of wingless and winged aphids (27). They are also exposed to a variety of biotic and abiotic stressors (e.g., natural predators, temperature, drought, fungi, and pesticides) and are able to rapidly adapt to environmental changes and new host plants (55). The expansion of IAPs could be a contributing factor to the phenotypic plasticity and stress resilience of aphids. For instance, they could be involved in the switch from wingless to winged aphids that is dependent on the inhibition of flight muscle degeneration, a physiological process for which some evidence was presented that it is apoptotic (29). Also, the expression of IAPs upon environmental stress could be a mechanism to support survival under adverse conditions, while, in parallel, the aphids adapt to the changed environment, thus explaining their amazing plasticity. Rapid IAP induction has also been demonstrated in the oyster *C. gigas* (54) upon exposure to a range of environmental stressors. Interestingly, phylloxera shares the polyphenism trait with true aphids. It is worth noting that, while IAP expansion might be involved in aphid-specific polyphenisms, it does not seem to be a hallmark of all arthropod polyphenisms. Indeed, even though *A. mellifera*, *L. migratoria*, or *D. pulex* present well-known polyphenisms (56, 57), they show no IAP expansion.

Future work will allow us to discriminate these possibilities and determine to what extent the observed IAP expansion contributes to aphid immunity or the prominent phenotypic plasticity observed in the aphid lineage.

Materials and Methods

Putative Apoptosis-Related Proteins Identification. In order to identify the *A. pisum* apoptosis-related proteins, we selected only insects in which pro- (caspases and adaptor protein) and antiapoptotic (IAP family members) protein homologs are well characterized (i.e., for which expert annotation and manual curation, cloning and sequencing, and, eventually, functional characterization were available) (13–21, 33, 46). Amino acid sequences were retrieved from the NCBI database (*SI Appendix*, Table S4) and used as a query to perform Basic Local Alignment Search Tool Protein (BLASTP) searches against the NCBI *A. pisum* genome. An Expected-value (E-value) cutoff of 0.1 was used to account for the large differences between species. The protein domains were predicted using the InterProScan software version 77.0 (58). Proteins were identified as caspases or IAPs when they had at least one CASc or one BIR domain, respectively.

We used the same procedure to identify and annotate the caspases and IAPs of an additional 10 aphid genomes and the aphid-related grapevine Phylloxera (*Daktulosphaira vitifoliae*). The latest annotation for each of these genomes was obtained either from the NCBI or from the AphidBase (https://bipaa.genouest.org/is/) databases. The complete repertoires of pro- and antiapoptotic proteins in the aphid lineage are listed in the *SI Appendix*, Tables S2 and S3, respectively.

Phylogenetic Reconstruction and Protein Annotation. *A. pisum* putative caspases and IAPs were further annotated by investigating their phylogenetic relationships with the well-characterized apoptosis-related proteins used for their identification, using phylogenetic reconstruction. Due to the divergence between apoptosis-related proteins, in terms of sequence length and domain composition/repetition, we used the isolated CASc or BIR domains of each caspase or IAP candidate, respectively, rather than the complete protein sequence. Individual domain boundaries were determined using the InterProScan software version 77.0 (58). For IAPs, BIR domains were numbered relative to their respective position in the protein sequence starting from the N terminus; for example, when two BIR domains were present in the protein, they were designated as BIR_1/2 and BIR_2/2. Phylogenetic trees were built using the Bayesian and the maximum likelihood estimation methods (fully described in the *SI Appendix, Supplementary Materials and Methods*).

Aphid Sampling. Aphids used in this study were obtained from a parthenogenetic clone (LL01) of *A. pisum* Harris containing only the primary endosymbiont *B. aphidicola*. Strictly parthenogenetic aphid matrilines were reared and synchronized as previously described (31). For RT-PCR experiments, synchronized aphids were collected at N1 (first instar; 1 d old), N2 (second instar; 3 d old), N3 (third instar; 5 d old), and N4 (fourth instar; 7 d old) nymphal stages and at A9 (9 d old), A15 (15 d old), and A23 (23 d old) adult stages. Aphids were subsequently pooled and used to perform total RNA extractions. For qRT-PCR experiments, synchronized aphids were collected at N3, N4, A9, A15, and A23 life stages and subsequently used for tissue dissection.

RT-PCR. Total RNA was extracted using the RNeasy Mini Kit (Qiagen, Hilden, Germany) and treated with DNase I (Promega). First-strand cDNA was then synthetized using the SuperScript III First-Strand Synthesis System (Invitrogen) with oligo(dT)20 primers. PCR was performed on a T100 Thermal Cycler (BioRad) using 1 μg cDNAs and the Taq'Ozyme polymerase (Ozyme) according to the manufacturer's instructions and as previously described (59). All of the primers used in this work are listed in the *SI Appendix*, Table S5. The expected PCR amplicon sizes and sequences were controlled by gel electrophoresis and Sanger sequencing.

Spatiotemporal qRT-PCR Analysis. Tissues were surgically isolated in ice-cold isosmotic buffer A (0.025 M KCl, 0.01 M MgCl2, 0.25 M sucrose, and 0.035 M Tris·HCl, pH 7.5) under 25× to 40× magnification with a MDG-17 stereomicroscope (Leica). They were then collected using fine forceps Dumont type 5 Dumoxel (Electron Microscopy Science) with the exception of bacteriocytes, which were collected with a Pasteur glass pipette attached to a peristaltic pump MINIPULS 3 (Gilson). To guarantee sufficient extracted RNA from each tissue, bacteriocytes and gut were collected from 30 aphids, embryonic chains from 10 to 20 aphids depending on the life stages, head from 50 aphids, and carcass from 10 aphids.

Total RNA extraction and first-strand cDNA preparation were conducted as described above. Real-time RT-PCR reactions were performed as described in the *SI Appendix, Supplementary Materials and Methods*.

3D Modeling and Molecular Docking. The models of the aphid BIR domains were built using the SWISS-MODEL server (60) and energy minimized with the Maestro version 11.2 software (Schrödinger, LLC). The AVPI tetrapeptide was built using the geometry of the AVPI tetrapeptide from the IAP-antagonist Smac, a typical IBM similar to the ones found in caspases and other IAP antagonists, in complex with X-linked inhibitor of apoptosis XIAP BIR2 domain (Protein Data Bank [PDB] archive identification: 4j46) (61). The AVPI tetrapeptide was then docked into the IBM groove of aphid BIR domains. The full procedure is described in the *SI Appendix, Supplementary Materials and Methods*.

Gateway Cloning. Five pea aphid IAPs were selected based on their domain composition and expression patterns and their nucleotide sequences codon-optimized for expression in *D. melanogaster*. The chemically synthesized sequences (obtained from Integrated DNA technology, https://eu.idtdna.com/) were PCR amplified using primers containing the attB1 and attB2 gateway tails at the 5′ end of the forward and reverse primer, respectively (*SI Appendix*, Table S5). The PCR reactions were performed using the Phusion High-Fidelity DNA Polymerase (Thermo Fisher Scientific) according to the manufacturer's specifications. The PCR products were cloned into the pUGa vector, an expression vector suitable for heterologous expression in *D. melanogaster*, using a two-step Gateway cloning protocol as previously described (62). The full procedure for Gateway cloning is described in the *SI Appendix, Supplementary Materials and Methods*.

Heterologous Expression and Phenotypic Analyses. The antiapoptotic activity of *A. pisum* IAPs was tested using the *Drosophila* eye-based screening assay developed by Hay et al. (43) and previously used to test pro- or antiapoptotic potential of proteins in *D. melanogaster* (a full list of references is in the *SI Appendix*). Transgenic *D. melanogaster* harboring the UAS-IAP constructs (see above) were generated by GenetiVision as a service. Briefly, UAS constructs were introduced into the VK31 landing site (chromosome 3) using PhiC31-mediated site-specific insertion (63). Two to three independent transgenic lines were generated per transgene. To test antiapoptotic activity of *A. pisum* IAPs, the following *D. melanogaster* genotypes were established: GMR-GAL4/+;UAS-*iapx*/GMR-*rpr* with *iapx* being either one of the five *A. pisum* IAPs or *D. melanogaster* IAP1 (DIAP1, positive control for rescue). GMR-GAL4/+;+/GMR-*rpr* was used to determine maximum effect on eye size of *rpr*-induced apoptosis. GMR-rpr, GMR-GAL4, and UAS-DIAP1 *D. melanogaster* stocks were obtained from the Bloomington *Drosophila* Stock Center.

Images of heads of 10 randomly selected control flies (only the gene *rpr* is expressed) and 10 randomly selected rescue flies per line (the gene *rpr* is coexpressed with a pea aphid *iap* gene) were acquired with Cell^D software (Olympus Life Science) using an Olympus XC30 camera mounted on an Olympus SZX12 inverted microscope. Head and eye surfaces were measured using the ImageJ software (https://imagej.nih.gov/ij/), and eye surface/head surface ratios were calculated for each gene. The control and rescue flies were also analyzed by SEM (*SI Appendix, Supplementary Materials and Methods*).

Statistics. Data normality and homoscedasticity assumptions were checked with the Shapiro–Wilk and Bartlett tests, respectively. For the expression analysis, experimental data were analyzed by ANOVA followed by post hoc multiple comparisons using Tukey's honestly significant difference (HSD) test. For the heterologous expression analysis, experimental data were analyzed using the Mann–Whitney *U* test. All statistical analyses were carried out using R software version 3.1.1 (https://www.r-project.org/) with values of $P < 0.05$ considered significant.

Data Availability. All study data are included in the article and supporting information.

ACKNOWLEDGMENTS. We thank Mattias Winant for his help with the *D. melanogaster* work; Gaël Le Trionnaire, Fabrice Legeai, and Denis Tagu for their advice on aphid genomic resources; and Céline Brochier Armanet for suggestions on phylogenetic reconstruction. This work was supported by the Institut National de Recherche pour l'Agriculture, l'Alimentation et l'Environnement; INSA (Institut National des Sciences Appliquées), Lyon; the French ANR-16-CE02-0014 (HMicMac) program grant; and KU Leuven grant C14/17/099. INSA-Lyon supported P.C. with an Invited Professorship.

1. L. Galluzzi *et al*., Molecular mechanisms of cell death: Recommendations of the nomenclature committee on cell death 2018. *Cell Death Differ.* **25**, 486–541 (2018).
2. Y. Fuchs, H. Steller, Live to die another way: Modes of programmed cell death and the signals emanating from dying cells. *Nat. Rev. Mol. Cell Biol.* **16**, 329–344 (2015).
3. E. H. Baehrecke, How death shapes life during development. *Nat. Rev. Mol. Cell Biol.* **3**, 779–787 (2002).
4. J. Pellettieri, A. Sánchez Alvarado, Cell turnover and adult tissue homeostasis: From humans to planarians. *Annu. Rev. Genet.* **41**, 83–105 (2007).
5. F. Nainu, A. Shiratsuchi, Y. Nakanishi, Induction of apoptosis and subsequent phagocytosis of virus-infected cells as an antiviral mechanism. *Front. Immunol.* **8**, 1220 (2017).
6. P. Fuentes-Prior, G. S. Salvesen, The protein structures that shape caspase activity, specificity, activation and inhibition. *Biochem. J.* **384**, 201–232 (2004).
7. R. C. Taylor, S. P. Cullen, S. J. Martin, Apoptosis: Controlled demolition at the cellular level. *Nat. Rev. Mol. Cell Biol.* **9**, 231–241 (2008).
8. J. Berthelet, L. Dubrez, Regulation of apoptosis by inhibitors of apoptosis (IAPs). *Cells* **2**, 163–187 (2013).
9. D. Vasudevan, H. D. Ryoo, Regulation of cell death by IAPs and their antagonists. *Curr. Top. Dev. Biol.* **114**, 185–208 (2015).
10. M. Ribeiro Lopes, N. Parisot, P. Callaerts, F. Calevro, "Genetic diversity of the apoptotic pathway in insects" in *Evolutionary Biology Book Series: Evolution, Origin of Life, Concepts and Methods*, P. Pontarotti, Ed. (Springer Nature Switzerland AG, 2019), pp. 253–285.
11. M. Orme, P. Meier, Inhibitor of apoptosis proteins in *Drosophila*: Gatekeepers of death. *Apoptosis* **14**, 950–960 (2009).

12. J. Chai *et al*., Molecular mechanism of Reaper-Grim-Hid-mediated suppression of DIAP1-dependent Dronc ubiquitination. *Nat. Struct. Biol.* **10**, 892–898 (2003).
13. A. Accorsi, A. Zibaee, D. Malagoli, The multifaceted activity of insect caspases. *J. Insect Physiol.* **76**, 17–23 (2015).
14. J. Courtiade, Y. Pauchet, H. Vogel, D. G. Heckel, A comprehensive characterization of the caspase gene family in insects from the order Lepidoptera. *BMC Genomics* **12**, 357 (2011).
15. N. Huang, S. Civciristov, C. J. Hawkins, R. J. Clem, SfDronc, an initiator caspase involved in apoptosis in the fall armyworm *Spodoptera frugiperda*. *Insect Biochem. Mol. Biol.* **43**, 444–454 (2013).
16. J. Y. Zhang *et al*., The genomic underpinnings of apoptosis in the silkworm, *Bombyx mori*. *BMC Genomics* **11**, 611 (2010).
17. W. T. Liao, Y. Yang, X. F. Wu, Expression and functional analysis of an inhibitor of apoptosis protein from *Trichoplusia ni*. *Biochem. Biophys. Res. Commun.* **293**, 675–679 (2002).
18. C. G. Hebert, J. J. Valdes, W. E. Bentley, Investigating apoptosis: Characterization and analysis of *Trichoplusia ni*-caspase-1 through overexpression and RNAi mediated silencing. *Insect Biochem. Mol. Biol.* **39**, 113–124 (2009).
19. Z. Yang *et al*., SfDredd, a novel initiator caspase possessing activity on effector caspase substrates in *Spodoptera frugiperda*. *PLoS One* **11**, e0151016 (2016).
20. D. Yang, L. Chai, J. Wang, X. Zhao, Molecular cloning and characterization of Hearm caspase-1 from *Helicoverpa armigera*. *Mol. Biol. Rep.* **35**, 405–412 (2008).
21. R. J. Cerio, R. Vandergaast, P. D. Friesen, Host insect inhibitor-of-apoptosis SfIAP functionally replaces baculovirus IAP but is differentially regulated by its N-terminal leader. *J. Virol.* **84**, 11448–11460 (2010).
22. R. J. Clem, The role of apoptosis in defense against baculovirus infection in insects. *Curr. Top. Microbiol. Immunol.* **289**, 113–129 (2005).
23. S. Tsuzuki, M. Iwami, S. Sakurai, Ecdysteroid-inducible genes in the programmed cell death during insect metamorphosis. *Insect Biochem. Mol. Biol.* **31**, 321–331 (2001).
24. B. Bryant, M. C. Ungerer, Q. Liu, R. M. Waterhouse, R. J. Clem, A caspase-like decoy molecule enhances the activity of a paralogous caspase in the yellow fever mosquito, *Aedes aegypti*. *Insect Biochem. Mol. Biol.* **40**, 516–523 (2010).
25. B. Misof *et al*., Phylogenomics resolves the timing and pattern of insect evolution. *Science* **346**, 763–767 (2014).
26. S. Shigenobu, H. Watanabe, M. Hattori, Y. Sakaki, H. Ishikawa, Genome sequence of the endocellular bacterial symbiont of aphids *Buchnera* sp. APS. *Nature* **407**, 81–86 (2000).
27. International Aphid Genomics Consortium, Genome sequence of the pea aphid *Acyrthosiphon pisum*. *PLoS Biol.* **8**, e1000313 (2010).
28. F. Calevro, D. Tagu, P. Callaerts, *Acyrthosiphon pisum*. *Trends Genet.* **35**, 781–782 (2019).
29. H. Feng *et al*., Flight muscles degenerate by programmed cell death after migration in the wheat aphid, *Sitobion avenae*. *BMC Res. Notes* **12**, 672 (2019).
30. I. Sprawka, S. Goławska, T. Parzych, H. Sytykiewicz, P. Czerniewicz, Apoptosis induction by concanavalin A in gut cells of grain aphid. *Arthropod-Plant Interact.* **9**, 133–140 (2015).
31. P. Simonet *et al*., Bacteriocyte cell death in the pea aphid/*Buchnera* symbiotic system. *Proc. Natl. Acad. Sci. U.S.A.* **115**, E1819–E1828 (2018).
32. Y. Li, H. Park, T. E. Smith, N. A. Moran, Gene family evolution in the pea aphid based on chromosome-level genome assembly. *Mol. Biol. Evol.* **36**, 2143–2156 (2019).
33. B. Bryant, C. D. Blair, K. E. Olson, R. J. Clem, Annotation and expression profiling of apoptosis-related genes in the yellow fever mosquito, *Aedes aegypti*. *Insect Biochem. Mol. Biol.* **38**, 331–345 (2008).
34. E. V. Kriventseva *et al*., OrthoDB v10: Sampling the diversity of animal, plant, fungal, protist, bacterial and viral genomes for evolutionary and functional annotations of orthologs. *Nucleic Acids Res.* **47**, D807–D811 (2019).
35. S. J. Snipas, M. Drag, H. R. Stennicke, G. S. Salvesen, Activation mechanism and substrate specificity of the *Drosophila* initiator caspase DRONC. *Cell Death Differ.* **15**, 938–945 (2008).
36. A. G. Fraser, C. James, G. I. Evan, M. O. Hengartner, *Caenorhabditis elegans* inhibitor of apoptosis protein (IAP) homologue BIR-1 plays a conserved role in cytokinesis. *Curr. Biol.* **9**, 292–301 (1999).
37. F. Cossu, M. Milani, E. Mastrangelo, D. Lecis, Targeting the BIR domains of inhibitor of apoptosis (IAP) proteins in cancer treatment. *Comput. Struct. Biotechnol. J.* **17**, 142–150 (2019).
38. P. D. Mace, S. Shirley, C. L. Day, Assembling the building blocks: Structure and function of inhibitor of apoptosis proteins. *Cell Death Differ.* **17**, 46–53 (2010).
39. B. P. Eckelman, G. S. Salvesen, The human anti-apoptotic proteins cIAP1 and cIAP2 bind but do not inhibit caspases. *J. Biol. Chem.* **281**, 3254–3260 (2006).
40. A. Schmid, B. Schindelholz, K. Zinn, Combinatorial RNAi: A method for evaluating the functions of gene families in *Drosophila*. *Trends Neurosci.* **25**, 71–74 (2002).
41. P. Sapountzis *et al*., New insight into the RNA interference response against cathepsin-L gene in the pea aphid, *Acyrthosiphon pisum*: Molting or gut phenotypes specifically induced by injection or feeding treatments. *Insect Biochem. Mol. Biol.* **51**, 20–32 (2014).
42. A. H. Brand, N. Perrimon, Targeted gene expression as a means of altering cell fates and generating dominant phenotypes. *Development* **118**, 401–415 (1993).
43. B. A. Hay, D. A. Wassarman, G. M. Rubin, *Drosophila* homologs of baculovirus inhibitor of apoptosis proteins function to block cell death. *Cell* **83**, 1253–1262 (1995).
44. F. Legeai *et al*., AphidBase: A centralized bioinformatic resource for annotation of the pea aphid genome. *Insect Mol. Biol.* **19**, 5–12 (2010).
45. C. Rispe *et al*., The genome sequence of the grape phylloxera provides insights into the evolution, adaptation, and invasion routes of an iconic pest. *BMC Biol.* **18**, 90–115 (2020).
46. X. R. Wang *et al*., The functions of caspase in whitefly *Bemisia tabaci* apoptosis in response to ultraviolet irradiation. *Insect Mol. Biol.* **27**, 739–751 (2018).
47. S. M. Srinivasula, J. D. Ashwell, IAPs: What's in a name? *Mol. Cell* **30**, 123–135 (2008).
48. A. Koto, E. Kuranaga, M. Miura, Temporal regulation of *Drosophila* IAP1 determines caspase functions in sensory organ development. *J. Cell Biol.* **187**, 219–231 (2009).
49. J. R. Huh *et al*., The *Drosophila* inhibitor of apoptosis (IAP) DIAP2 is dispensable for cell survival, required for the innate immune response to gram-negative bacterial infection, and can be negatively regulated by the reaper/hid/grim family of IAP-binding apoptosis inducers. *J. Biol. Chem.* **282**, 2056–2068 (2007).
50. Y. Kaplan, L. Gibbs-Bar, Y. Kalifa, Y. Feinstein-Rotkopf, E. Arama, Gradients of a ubiquitin E3 ligase inhibitor and a caspase inhibitor determine differentiation or death in spermatids. *Dev. Cell* **19**, 160–173 (2010).
51. S. Blanc, M. Drucker, M. Uzest, Localizing viruses in their insect vectors. *Annu. Rev. Phytopathol.* **52**, 403–425 (2014).
52. N. M. Gerardo *et al*., Immunity and other defenses in pea aphids, *Acyrthosiphon pisum*. *Genome Biol.* **11**, R21 (2010).
53. C. M. Adema *et al*., Whole genome analysis of a schistosomiasis-transmitting freshwater snail. *Nat. Commun.* **8**, 15451 (2017).
54. G. Zhang *et al*., The oyster genome reveals stress adaptation and complexity of shell formation. *Nature* **490**, 49–54 (2012).
55. J. C. Simon, J. Peccoud, Rapid evolution of aphid pests in agricultural environments. *Curr. Opin. Insect Sci.* **26**, 17–24 (2018).
56. S. J. Simpson, G. A. Sword, N. Lo, Polyphenism in insects. *Curr. Biol.* **21**, R738–R749 (2011).
57. Z. Ye, C. Molinier, C. Zhao, C. R. Haag, M. Lynch, Genetic control of male production in *Daphnia pulex*. *Proc. Natl. Acad. Sci. U.S.A.* **116**, 15602–15609 (2019).
58. P. Jones *et al*., InterProScan 5: Genome-scale protein function classification. *Bioinformatics* **30**, 1236–1240 (2014).
59. P. Simonet *et al*., Disruption of phenylalanine hydroxylase reduces adult lifespan and fecundity, and impairs embryonic development in parthenogenetic pea aphids. *Sci. Rep.* **6**, 34321 (2016).
60. A. Waterhouse *et al*., SWISS-MODEL: Homology modelling of protein structures and complexes. *Nucleic Acids Res.* **46**, W296–W303 (2018).
61. C. Lukacs *et al*., The structure of XIAP BIR2: Understanding the selectivity of the BIR domains. *Acta Crystallogr. D Biol. Crystallogr.* **69**, 1717–1725 (2013).
62. K. Hens *et al*., Automated protein-DNA interaction screening of *Drosophila* regulatory elements. *Nat. Methods* **8**, 1065–1070 (2011).
63. J. Bischof, R. K. Maeda, M. Hediger, F. Karch, K. Basler, An optimized transgenesis system for *Drosophila* using germ-line-specific phiC31 integrases. *Proc. Natl. Acad. Sci. U.S.A.* **104**, 3312–3317 (2007).